Journal of Experimental Botany, Vol. 70, No. 10 pp. 2637–2650, 2019
doi:10.1093/jxb/erz086 Advance Access Publication 1 March 2019
This paper is available online free of all access charges (see https://academic.oup.com/jxb/pages/openaccess for further details)

RESEARCH PAPER

Carotenoid biosynthesis and sequestration in red chilli pepper fruit and its impact on colour intensity traits

Harriet M. Berry[1], Daniel V. Rickett[2], Charles J. Baxter[2], Eugenia M.A. Enfissi[1] and Paul D. Fraser[1,*]

[1] School of Biological Sciences, Royal Holloway, University of London, Egham, Surrey TW20 OEX, UK
[2] Syngenta, Jealott's Hill International Research Centre, Bracknell, Berkshire RG42 6EY, UK

* Correspondence: p.fraser@rhul.ac.uk

Received 11 October 2018; Editorial decision 11 February 2019; Accepted 20 February 2019

Editor: Ariel Vicente, CONICET-National University of La Plata, Argentina

Abstract

The exploitation of diverse natural variation has been a key progenitor of crop breeding over the last decade. However, commercial practice is now turning to the use of accessions with less extreme phenotypes as genetic donors. In the present study, the carotenoid formation in a red-fruited discovery panel of *Capsicum annuum* (chilli pepper) has been characterized. The data indicated that colour intensity correlated with the amount of capsanthin and its esters, along with transcript levels of the 1-deoxy-D-xylulose 5-phosphate synthase (*DXS*) and phytoene synthase-1 (*PSY*-1) genes. Quantification of carotenoids through development and ripening suggested the presence of separate biosynthesis and accumulation phases. Subplastid fractionation demonstrated the differential sequestration of pigments in high- and low-intensity lines and revealed the PSY protein to be most active in the membrane fractions when abundance was highest in the fibril fractions. Carotenoid accumulation was associated with the esterification of xanthophylls, expression of a putative carotenoid acyl transferase, and increased fibril content within the plastid. Interrogation of TEM images and carotenoid analysis of subplastid fractions suggest that the plastoglobuli are likely to be the progenitor of the characteristic fibrils found in pepper fruit. Collectively, these data provide an insight into the underpinning molecular, biochemical, and cellular mechanisms associated with the synthesis and sequestration of carotenoids in chromoplast-containing fruits, in addition to providing potential tools and resources for the breeding of high red colour intensity pepper varieties.

Keywords: *Capsicum*, carotenoids, colour, isoprenoids, plastids, sequestration.

Introduction

Tomato (*Solanum lycopersicum*) has become the model crop species for all fleshy fruit crops, with vast genetic and biochemical resources now available. Translating these resources and knowledge to other fruit crops is a key objective for the scientific community. Peppers (*Capsicum annuum* L.), both sweet and chilli varieties, are, like tomato, members of the *Solanaceae* family and have a high economic value. It is presently estimated that world production of red chilli fruit is in the region of 3.0 Mt, having a price of US$200–400 t^{-1}, which is higher than tomato fruit (www.fao.org/faostat/en/#data/QV). Other similarities between tomato and *Capsicum* fruit include the transition from chloroplast- to chromoplast-containing tissues during ripening and the high carotenoid content in these chromoplast-containing fruit, which results in their characteristic red colour. It is the chromoplast organelle that is associated with the ability of these fruit tissues to accumulate carotenoid pigments.

In plants, carotenoids perform a variety of roles associated with their potent antioxidant activity and characteristic chromophore, including accessory photosynthetic pigments, free radical scavengers (Demmig-Adams and Adams, 2002; Wurtzel, 2019), and precursors of phytohormones such as abscisic acid (Ji *et al.*, 2014) and strigolactones (Alder *et al.*, 2012) (Fig. 1). Humans cannot synthesize carotenoids *de novo*; instead they must be acquired from the diet. The intake of fruit and vegetables rich in carotenoids has been shown from epidemiological and intervention studies to reduce the onset of chronic disease states, such as certain cancers, age-related macular degeneration, and cardiovascular diseases (Fraser and Bramley, 2004; Story *et al.*, 2010; Giuliano, 2017).

Carotenoid pigments are isoprenoid molecules and thus derived from the universal five carbon precursor isopentenyl pyrophosphate (IPP, C_5). In higher plants, they are synthesized in the plastid using IPP generated from the methylerythritol-4-phosphate (MEP) pathway (Fig. 1). Geranylgeranyl pyrophosphate (GGPP, C_{20}) is the prenyl lipid precursor utilized to form carotenes. Two molecules of GGPP are condensed in a head to tail manner by phytoene synthase (Fraser *et al.*, 2000). This reaction represents the first committed step in carotenoid formation. Phytoene undergoes a series of sequential desaturation (dehydrogenation) steps to yield lycopene via phytofluene, ζ-carotene, and neurosporene. Carotene isomerization, from *cis* to *trans* geometric configuration, is also an integral component of the sequence requiring two isomerases (Moise *et al.*, 2014). All-*trans* lycopene can be cyclized to α-carotene and β-carotene via the action of ε- and/or β-ring cyclases. In red tomato fruit, β-carotene is present but lycopene usually predominates. In contrast, the carotenoid pathway in *Capsicum* fruit extends to xanthophylls, particularly β-ionone ring-derived xanthophylls (Fig. 1), unlike the ε-ring- (α-carotene) derived xanthophylls found in chloroplast-containing tissues. The formation of xanthophylls in *Capsicum* species is initiated by the hydroxylation of β-carotene to form zeaxanthin. Epoxidation of zeaxanthin by the enzyme zeaxanthin epoxidase (ZEP) results in violaxanthin formation. This reaction sequence is reversible in nature through the action of violaxanthin de-epoxidase (VDE). Violaxanthin can also be converted to neoxanthin (Bouvier *et al.*, 2000). The end-products found in red *Capsicum* fruit are the red pigments capsorubin and capsanthin, the latter being the most abundant. To form capsanthin/capsorubin, the action of capsanthin/capsorubin synthase (CCS) is required (Lefebvre *et al.*, 1998). The gene encoding this enzyme shows strong homology to the carotene cyclase(s) and it is postulated that the enzyme can also generate β-carotene in the fruit tissues (Hugueney *et al.*, 1996). The CCS enzyme is responsible for generating the characteristic cyclopentane or κ-ring found in the *Capsicum* carotenoid pigments, capsanthin and capsorubin (Gómez-García and Ochoa-Alejo, 2013).

Phytoene synthase is a key regulator in the biosynthesis of carotenoids and influences flux into the carotenoid pathway (Fraser *et al.*, 2002). It is postulated that phytoene synthase (*PSY*) expression is under the influence of pathway products and intermediates via feedback mechanisms that await full elucidation (Kachanovsky *et al.*, 2012; Enfissi *et al.*, 2017), and its activity is believed to be dependent on isoforms present and the intracellular location of these proteins (Shumskaya *et al.*, 2012). In Arabidopsis, there is one isoform, tomato has three isoforms (leaf, fruit, and root), and pepper has been found to have two (Thorup *et al.*, 2000; Kilcrease *et al.*, 2015). There have been reports of the PSY having differential levels of activity depending on its plastidial location (Fraser *et al.*, 2002; Welsch *et al.*, 2018), but more information specific to *Capsicum* is needed (Rodriguez-Concepcion *et al.*, 2018).

In addition to their biosynthesis, carotenoids are also sequestrated in the plastid organelle. Carotenoids are extremely hydrophobic and are stored in specialized structures in the chromoplast called plastoglobuli (PGs; van Wijk and Kessler, 2017). In *Capsicum*, the xanthophylls are esterified to allow more efficient storage and increased stability (Hornero-Méndez and Mínguez-Mosquera, 1994, 2000). The type of PGs accumulated in chromoplasts can differ greatly. Globular PGs are found in tomato (Camara *et al.*, 1995; Vishnevetsky, 1999); however, in pepper, as well as globular PGs, unique, specialized fibrillin structures (fibrils) develop to sequestrate the carotenoids (Deruère *et al.*, 1994). It has been shown that specific chromoplast shapes correlate with carotenoid compositions (Kilcrease *et al.*, 2013) and that the carotenoid content can be elevated when the levels of fibillin increased (Simkin *et al.*, 2007). Additionally, there is some evidence to suggest that fibrils arise from PGs in pepper, cucumber, and greater celandine (Simpson and Lee, 1976; Prebeg *et al.*, 2006*a*, *b*). The sequestration of carotenoids into PGs not only allows them to be stored more efficiently but also acts as a form of regulation whereby partioning carotenoids into compartmentalized structures physically separates them from biosynthetic enzymes (Lu *et al.*, 2006; Enfissi *et al.*, 2010; Nogueira *et al.*, 2013).

The ability of carotenoids to confer nutritional and aesthetic quality to fruits has made them a target for plant breeding programmes. Over the last decade, crop improvement programmes have focused on the exploitation of diverse natural variation to capture features from 'exotic' allelic diversity. However, this approach has frequently resulted in detrimental effects due to genetic drag. The improvements to traits have typically been moderate and unstable. Alternatively, most commercial activities are now using closely related accessions that do not show the phenotypic extremes typically observed when using wild 'exotic' relatives. In this way, the favourable agronomic properties are already fixed and heterosis can be fully exploited (Baenziger *et al.*, 2017).

Further understanding of the sequestration mechanisms in fruit chromoplasts is necessary to provide new insights related to carotenoid modification and PG formation (Wurtzel, 2019). Furthermore, previous studies of colour in the pepper fruit do not always predict carotenoid accumulation in pepper (Guzman *et al.*, 2010; Rodriquez-Uribe *et al.*, 2012). Therefore, more detailed descriptions of carotenoid ester and fibril formation are valuable and could be transferred to other crop plants that accumulate carotenoids at high levels in the esterified form. Despite the comparative rapid advances made with the formation of carotenoids in tomato, the transfer of information to *Capsicum* fruit has not been starightforward, and a gap in our knowledge exists with respect to *Capsicum* fruit (Gómez-García and Ochoa-Alejo, 2013).

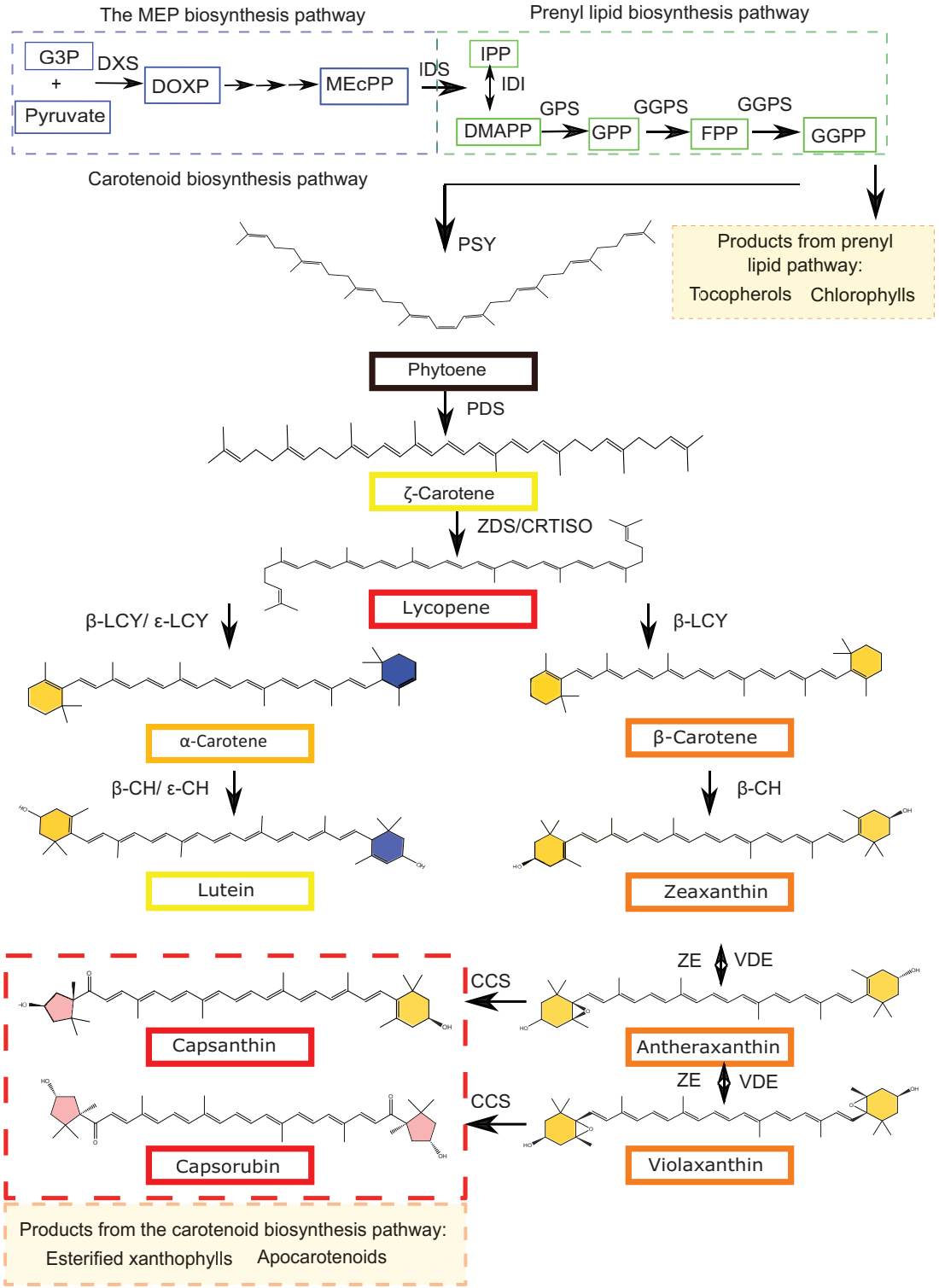

Fig. 1. The plastidial isoprenoid biosynthesis pathway in *Capsicum*. The MEP pathway (blue) receives substrates, G3P and pyruvate, from primary metabolism and delivers IPP to the prenyl lipid pathway (green). Phytoene, the first carotenoid in the carotenoid pathway, is synthesized from eight IPP units in the prenyl lipid pathway. The carotenoid biosynthesis pathway is split into two distinct branches: the α- and β-branch. The α-branch containing the ε-ring carotenoids is shown on the left (blue rings) and the β-branch is shown on the right. The transition from carotene to xanthophyll is characterized by the addition of a hydroxyl group to the end rings. The compounds capsanthin and capsorubin with κ end groups are unique to *Capsicum* and are represented by the red shading in the xanthophyll pathway. The products from the prenyl lipid and carotenoid pathway relevant to this study can be found in the orange boxes. Abbreviations: MEP, 2-C-methyl-D-erythritol 4-phosphate; G3P, D-glyceraldehyde 3-phosphate; DOXP, 1-deoxy-D-xylulose 5-phosphate; DXS, DOXP synthase; MEcPP, 2-C-methyl-D-erythritol-2,4-cylcopyrophosphate; IPP, isopentyl disphosphate; DMAPP, dimethylallyl diphosphate; IDS, IPP/DMAPP synthase; IDI, IPP/DMAPP isomerase; GPP, geranylpyrophospahte; GPS, GPP synthase; FPP, farnesylpyrophosphate; GGPP, geranylgeranylpyrophosphate; GGPS, GGPP synthase; PSY, phytoene synthase; PDS, phytoene desaturase; ZDS, ζ-carotene desaturase; CRTISO, carotenoid isomerase; LCY-β, lycopene β-cyclase; LCY-ε, lycopene ε-cyclase; β-CH, β-carotene hydroxylase; ε-CHY, ε-carotene hydroxylase; ZE, zeaxanthin epoxidase; VDE, violaxanthin de-epoxidase; CCS, capsanthin capsorubin synthase.

The aim of the present study was to characterize carotenoid formation in a *Capsicum annuum* discovery panel which display similar agronomic and colour properties, but differ in the intensity of red coloration found in ripe fruit. The classification of colour intensities was based on breeders' observations; the objective was to provide sound quantitative data to validate the observations and to provide information and valuable insights into the fundamental aspects of carotenoid formation during fruit development and ripening at a molecular and cellular level, as well as elucidating suitable parents for future breeding programmes addressing red fruit colour intensity in *Capsicum*.

The molecular and biochemical characterization revealed: (i) the key progenitors for high colour (carotenoid) intensity in red chilli pepper; (ii) distinct phases for synthesis and sequestration of carotenoids during pepper fruit formation; and (iii) valuable insights into the subplastid intracellular organization of carotenoid synthesis and sequestration components in *Capsicum* fruit. This included PSY activity associated with the membrane fractions but inactive in the fibrils fraction, and the presence of an intermediate PG structure suggesting that fibrils form from PGs.

Materials and methods

Plant material

The chilli pepper lines used in this study were from a colour discovery panel supplied by Syngenta (Supplementary Table S1 at *JXB* online). The plants were greenhouse grown (25 °C day/15 °C night) from seed, and supplementary lighting was used (110 μmol m^{-2} s^{-1}; 16 h/8 h light/dark cycle). The plants were tagged at anthesis. The mature green stage was determined as 55 d post-anthesis, breaker (B) was tagged by the first appearance of red colour, and the stages analysed after were breaker plus 3 d (B+3), breaker plus 7 d (B+7), breaker plus 10 d (B+10), and breaker plus 14 d (B+14). Carotenoid data were collected over three crops.

Metabolite analysis

The analysis of carotenoids was carried out using HPLC-PDA (photodiode array), as described in detail by Fraser *et al.* (2000). Dried whole fruit, excluding the seeds, homogenized to fine powder (5 mg), was used as starting material and extracted with the chloroform/methanol method (Nogueira *et al.*, 2013). Identification of the carotenoids (and chlorophylls) was from the comparison between characteristic carotenoid (and chlorophyll) spectra displayed by authentic standards and co-chromatography. In addition, reference spectra from the literature were consulted (Britton *et al.*, 2004). Identification of the carotenoid esters was carried out using LC-MS, with the method described in Perez-Fons *et al.* (2011).

Molecular analysis

Gene expression analysis was carried out by the method described in Enfissi *et al.* (2010), with the difference that quantitative PCR (qPCR) was carryied out on cDNA created from RNA in a two-step reaction. Gene expression was calculated on relative expression. Primers can be found in Supplementary Table S4. A carotenoid acyl transferase from tomato (Ariizumi *et al.*, 2014; *Solyc01g098110*) was BLAST against the chilli pepper genome database (Qin *et al.*, 2014), and a putative, homologous sequence was identified.

Subplastid fractionation

The fractionation procedure was standardized with respect to the amount of starting material used and extract loaded onto the gradients. This enabled accurate comparison between the low- and high-intensity genotypes. Ripe fruit (20 g), using the method developed by Nogueira *et al.* (2016), were homogenized and the chromoplasts isolated. The chromoplasts were added to the bottom of a sucrose gradient and centrifuged at high speed (18 h). Fractions (1 ml) from the fractionation gradient were collected and, following extraction, the pigments were analysed using HPLC-PDA. The fractions were collected from the top (fraction 1) to the bottom of the tube, allowing quantification of the carotenoids. Subplastidial fractions were pelleted and fixed in 2.5% glutaraldehyde and then subjected to TEM as described in Nogueira *et al.* (2013).

Protein analysis and enzyme assays

Proteins were extracted from the subplastidial fractions and separated by SDS–PAGE on a 12.5% gel (1.5 h). Proteins were transferred to a polyvinylidene difluoride (PVDF) membrane, and immunodetection of PSY, lycopene β-cyclase (LCY), β-carotene hydroxylase (β-CH), ZEP, Rubisco large subunit (RbcL), Tic40, fibrillin, and plastoglobulin-1 was carried out as described in Fraser *et al.* (1994). Enzyme assays were carried out on fractions using [^{3}H]GGPP as described in Fraser *et al.* (1994).

Statistical analysis

Kruskal–Wallis one-way non-parametric ANOVA was performed using Monte Carlo permutations (10 000) for *P*-value calculation. Conover–Iman post-hoc tests (α=0.05) were Bonferroni corrected. All univariate tests were two-tailed. The upper case letters represent the statistical group to which the lines belong.

Results and discussion

A colour discovery panel reveals a complex mixture of free and esterified carotenoids in ripe fruit

On the basis of phenotypic colour intensity, a discovery panel of 12 genotypes (designated R1–R12) was selected. The genotypes have previously been classified as low, medium, or high colour intensity lines (Supplementary Table S1).

The carotenoid contents of the ripe fruit were complex (Fig. 2), with capsanthin and its monoester and diester derivatives predominating in all cases. Capsanthin diesters were the most abundant carotenoids present, contributing to 40–80% of the total carotenoid content depending on the line (Fig. 2, peaks 27, 29, 30, 31, and 32). MS/MS data revealed that the fatty acid moieties attached to capsanthin were saturated fatty acids, such as lauric (C12:0), myristic (C14:0), and palmitic acids (C16:0) (Supplementary Table S2). This agrees with previously reported studies by Breithaupt and Schwack (2000) and Schweiggert *et al.* (2005), as well as more recent studies by Giuffrida *et al.* (2013) and Cervantes-Paz *et al.* (2014). Antheraxanthin was identified in the free form (Fig. 2, peak 7) and both mono- (peaks 10, 12, 13, and 16) and diesterified (peaks 20, 26, and 28) forms. Zeaxanthin was found in the free (Fig. 2, peak 9) and diesterified form (peaks 23, 24, 25, and 33). β-Cryptoxanthin (Fig. 2, peak 11), violaxanthin (peak 5), and neoxanthin (peak 6) were not esterified, while capsorubin was present as a diester (peaks 21 and 22). The carotenes phytoene (Fig. 2, peak 2) and phytofluene (peaks 3 and 4) were detected along with α-tocopherol (peak 1). Altogether ~31 carotenoids were identified.

The carotenoids present in all genotypes across the panel have been determined. The data are summarized in Fig. 3A–C

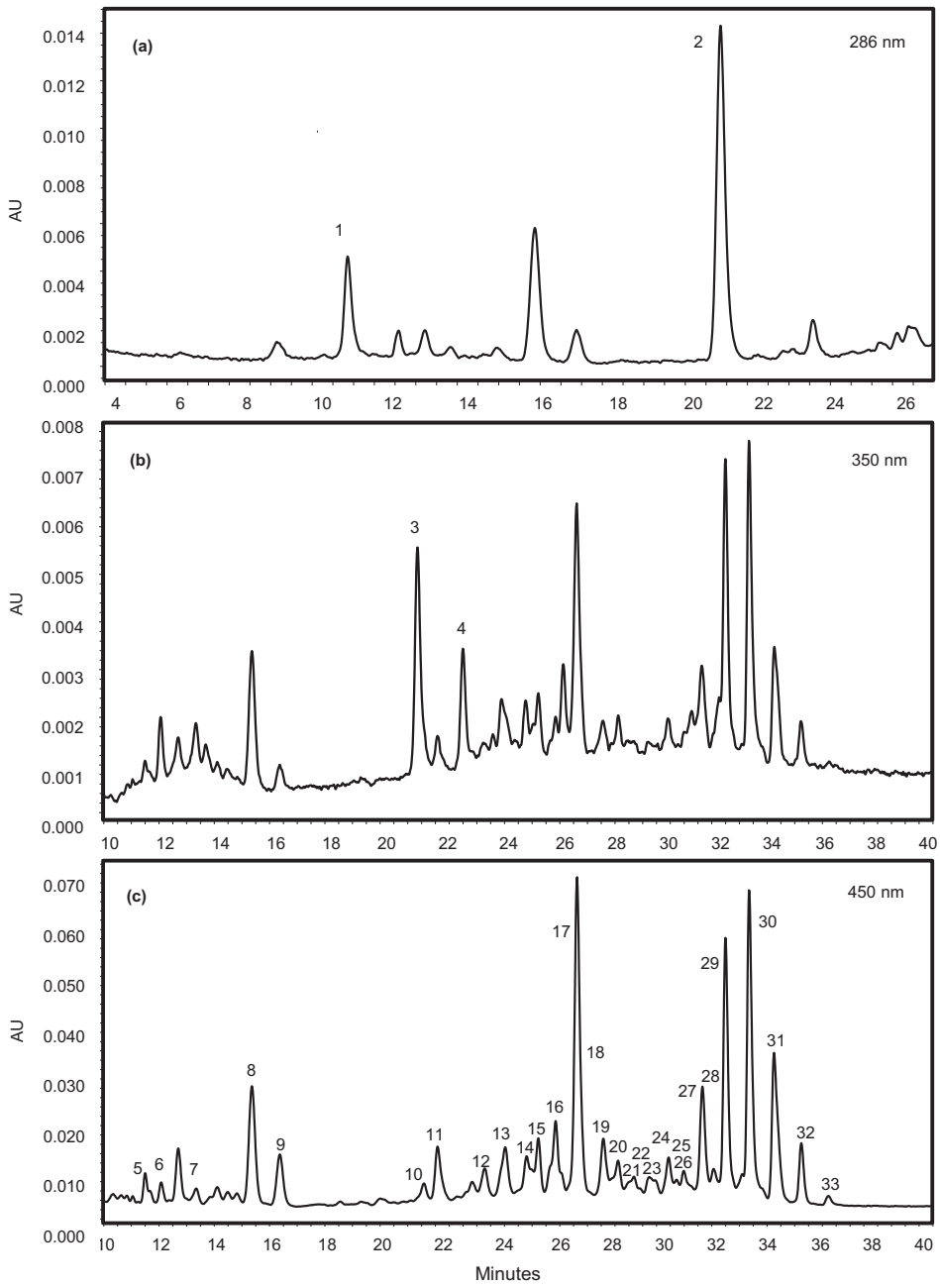

Fig. 2. Typical HPLC-PDA profile of carotenoids and their esters in a red ripe chilli pepper (R1). HPLC-PDA analysis was performed in order to identify and quantify the carotenoids present in the ripe fruit of red chilli pepper (R1, high-intensity phenotype). Identification of esterified carotenoids and their corresponding fatty acids was carried out using LC-MS (Supplementary Table S2). Observation wavelengths (A) 286 nm, (B) 350 nm, and (C) 450 nm. Assignment of peaks: 1-α-tocopherol; 2-phytoene; 3-phytofluene-1; 4-phytofluene-2; 5-violaxanthin; 6-neoxanthin; 7-anther; 8-capsanthin; 9-zea; 10-anther mono; 11-β-cryptoxanthin; 12-anther mono; 13-anther mono; 14-caps mono (C12:0); 15-caps mono (C14:0); 16-anther mono; 17-β-carotene-1; 18-caps mono (C16:0); 19-β-carotene-2; 20-anther di; 21-capsorubin di (C12:0-C12:0); 22-capsorubin di (C12:0-C14:0); 23-zea di (C12:0-C14:0); 24-zea di (C14:0-C14:0); 25-zea di; 26-anther di; 27-caps di (C12:0-C12:0); 28-anther di; 29-caps di (C12:0-C14:0); 30-caps di (C14:0-C14:0); 31-caps di (C14:0-C16:0); 32-caps di (C16:0-C16:0); 33-zea di (C16:0-C16:0). Key: zea, zeaxanthin; anther, antheraxanthin; caps, capsanthin; mono, monoester; di, diester.

and supported by Supplementary Fig. S1. Among all genotypes, levels of capsanthin (and its derivatives) were in the region of 2–6 mg g^{-1} DW. β-Carotene, antheraxanthin, phytoene, β-cryptoxanthin, zeaxanthin, and α-tocopherol were also present in amounts ranging from 1 mg g^{-1} to 1.5 mg g^{-1} DW, while phytofluene, capsorubin, violaxanthin, and neoxanthin were present at lower amounts (0.1–0.2 mg g^{-1} DW). The composition of pigments was similar in all genotypes. Comparison of the individual carotenoids of ripe fruit within the colour discovery panel revealed that high-intensity lines accumulated high levels of free carotenoids, which eventually become esterified. The accumulation of free capsanthin was most significant when compared with the other genotypes (0.5–0.6 mg g^{-1} DW) (Fig. 3A). R3, the low-intensity

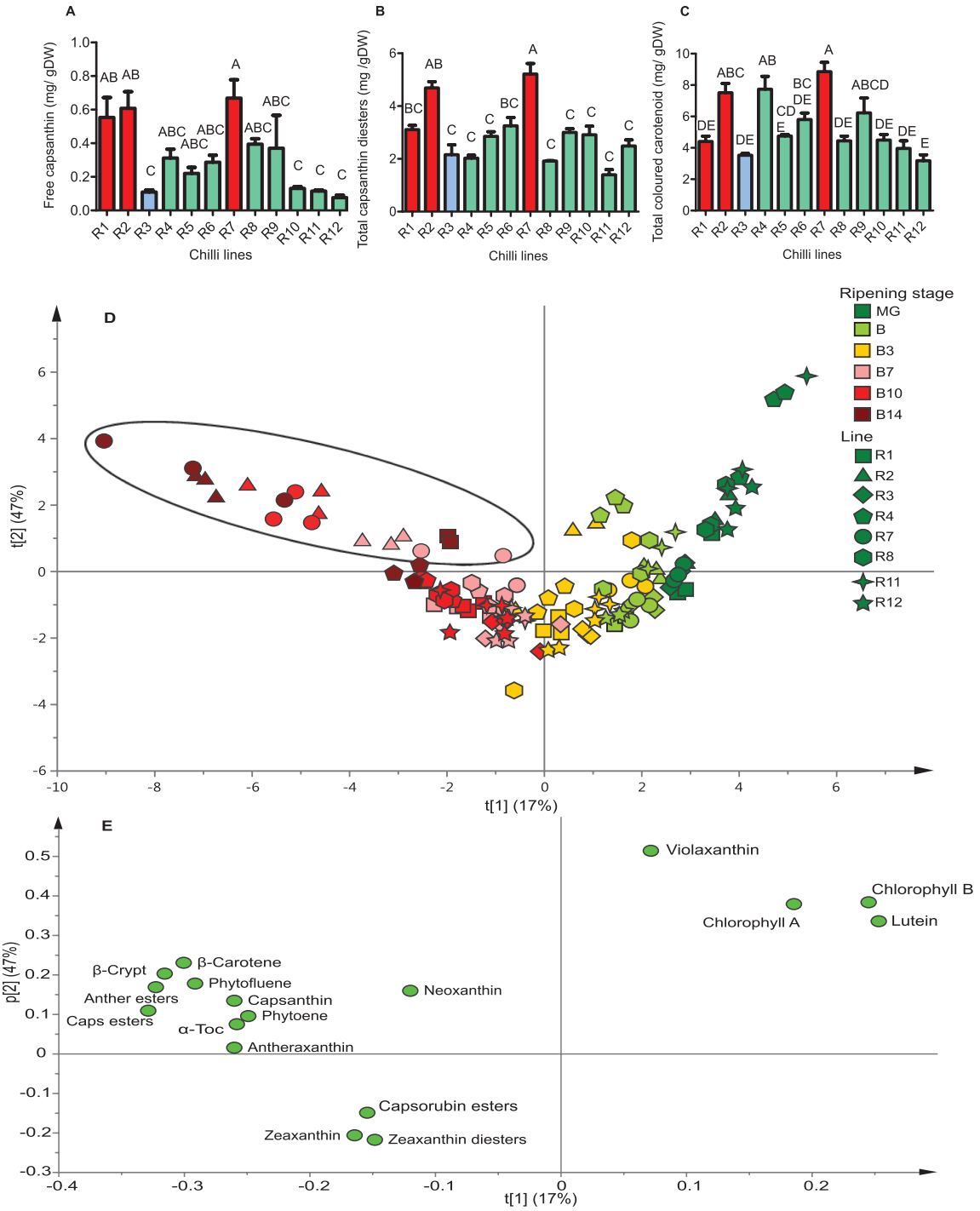

Fig. 3. Capsanthin, capsanthin diester, and total coloured carotenoid accumulation in red ripe chilli pepper and an overview of carotenoid accumulation during ripening. The carotenoids were quantified in 12 red ripe chilli pepper lines: (A) free capsanthin, (B) capsanthin diesters, and (C) total coloured carotenoid content. One-way ANOVA with Tukey post-hoc statistical analysis was carried out and lines were grouped based on their significance within the panel of lines ($P \leq 0.05$). Error bars represent ±SE ($n=3$). Key: (A–C) red, high intensity; green, medium intensity; blue, low intensity. Principal component analysis (PCA) was carried out on the pigments identified in selected lines to allow visualization of pigment accumulation throughout ripening: (D) PCA scores and (E) PCA loadings. The ripening stages were mature green (MG), breaker (B), breaker plus 3 d (B+3), breaker plus 7 d (B+7), breaker plus 10 d (B+10), and in R7 breaker plus 14 d (B+14). Key: R1, square; R2, triangle; R3, diamond; R4, pentagon; R7, circle; R8, hexagon; R11, four-point star; R12, five-point star; black ellipse, high-intensity phenotypes in ripe fruit. Abbreviations: anther, antheraxanthin; caps, capsanthin; zea, β-crypto, β-cryptoxanthin; α-toc, α-tocopherol.

line, displayed low levels of all carotenoids excluding capsorubin diesters and the isoprenoid α-tocopherol, which was not reduced when compared with the high-intensity germplasm (Supplementary Fig. S1).

Spearman's correlation was performed, and the amount of free capsanthin correlated more strongly to colour intensity phenotype ($R=0.794$, $P=0.003$; Fig. 3A) than the amount of capsanthin diesters accumulated ($R=0.672$, $P=0.019$; Fig.

3B). There was a weak correlation found between total carotenoid content and colour intensity phenotype (R=0.471, P=0.123; Fig. 3C). The determination of total carotenoid content illustrated that observational classification of fruit colour intensity does not necessary reflect total carotenoid content (Supplementary Table S1). This suggests that cellular or macromolecular structures could modify our perception of colour in these fruit.

The rate of biosynthesis and accumulation of carotenoids varied throughout fruit development and ripening of the different genotypes

Chilli pepper undergoes profound morphological and metabolic transformations during the ripening process as the chloroplast differentiates into a chromoplast. All genotypes displayed an increase in total carotenoid content as ripening proceeded, ranging from 3- to 25-fold from the mature green to ripe stages (Supplementary Table S3). In fleshy fruits such as tomato, watermelon, and papaya, lycopene accumulates, as cyclization is restricted and the early steps in the pathway are up-regulated (Fraser *et al.*, 2002). However, in chilli, a decline in lutein content and accumulation of capsanthin represented a shift in regulation from the α-branch of the biosynthetic pathway to the β-branch, resulting in *de novo* synthesis of capsanthin, zeaxanthin, capsorubin, antheraxanthin, and their esters, as well as β-cryptoxanthin, phytoene, and phytofluene.

Lutein was the most abundant carotenoid in mature green fruit, β-carotene and violaxanthin were also present, while neoxanthin, free antheraxanthin, and zeaxanthin were present at low levels. α-Tocopherol was also detected. Chl *a* was the most abundant chlorophyll. In all cases, the onset of ripening was marked by a decrease in lutein and chlorophylls and an increase in capsanthin, β-carotene, zeaxanthin, capsorubin, and antheraxanthin esters. Several genotypes showed a different pattern of carotenoid ester formation as ripening proceeded. Breaker stage revealed that initial ester formation favoured zeaxanthin in four lines (R1, R3, R8, and R12), while capsanthin ester formation was preferred by the high-intensity lines (R1, R2, and R7) (Supplementary Table S3; B). Red fruit (B+7) contained capsanthin esters accumulating as the most abundant carotenoid and having a similar content across all lines.

At the B+10 stage, the high-intensity line (R7) displayed a significantly higher content of all carotenoids, compared with the low-intensity line, R3. The exceptions were β-carotene, zeaxanthin, and capsorubin esters, being higher in R3. At the final stage of ripening (B+14), it was evident that the panel displayed variation in the rate of ripening. For example, R3, R8, and R12 had reached maturity and were senescing at B+14 stage (skin becoming dry and wrinkled), but R1, R2, R4, and R7 were still ripening, accumulating predominantly capsanthin (esters) and β-carotene. A comparison of the capsanthin ester content across genotypes at the final stage of ripening showed increased contents (up to 6 mg DW) in the high-intensity lines. A similar trend was observed for β-carotene and antheraxanthin esters at this late stage of ripening in the high-intensity lines. In order to define ripening rates with colour and specific carotenoids, principal component analysis (PCA) was carried out (Fig. 3D, E). The mature green stages clustered based on photosynthesis-related carotenoids and chlorophylls, whilst ripe fruit did so on the basis of ripening-related pigments, such as capsanthin (and its esters), phytoene, phytofluene, and α-tocopherol. Intermediate stages of ripening clustered on the contributions made by zeaxanthin and capsorubin (and their esters) (Fig. 3E). In the high-intensity lines, ripe fruit were all found in the top left quartile of the PCA, clustering separately on the basis of ripening-related pigments (Fig. 3D, black ellipse). The low- and medium-intensity lines clustered in the bottom left quartile of the PCA, with zeaxanthin and capsorubin the progenitors of the separation.

Xanthophyll ester formation appeared to be a key factor in the final colour intensity. Three lines were selected, based on differing colour intensity and ripening rate phenotypes. R1 and R7 have high intensity phenotypes but ripening rates are fast and slow, respectively. R3, however, has low colour intensity, but fast ripening. Comparisons revealed that the high-intensity lines accumulated capsanthin diesters in a linear manner throughout ripening (Fig. 4A, C), whereas the low-intensity line did not (Fig. 4B). The differing ripening rates between the lines and their effects on accumulation were also revealed. The R1 and R3 lines displayed a faster rate of ripening than the R7 line. This is apparent when comparing the transition between biosynthesis and accumulation; R1 and R3 experienced a transition around B+7, in contrast to R7 at B+14.

The abundance of capsanthin diesters in the fruit, and the fact that capsanthin has a red hue, strongly suggests that the concentration of capsanthin diesters at the later stages of ripening is responsible for the intensity of the red colour of the fruit (Hornero-Méndez and Mínguez-Mosquera, 2000). Logistically the data also highlight the need to analyse carotenoid esters in their true conjugated form if informative quantitative data are to be acquired. Also observed was a lack of absolute correlation between the carotenoid contents and the observational classifications made by breeders. This has also been found previously (Guzman *et al.*, 2010; Rodriguez-Uribe *et al.*, 2012). These findings suggest that other factors, such as carotenoid esterification and sequestration, besides ripe fruit capsanthin content can contribute to colour intensity phenotype and reflect the different backgrounds of the lines used in the discovery panel. In addition, precise quantitative analysis of carotenoid esters in their conjugated form is required to better characterize traits in fruits, especially if they are to form the basis of subsequent breeding programmes.

Expression of PSY-1 *and* DXS *is positively correlated with high colour intensity*

Carotenoid biosynthetic genes were selected based on their transcript profiles observed in the RNA sequencingdata described in Kim *et al.* (2014). Gene expression assays were performed to relate increased carotenogenesis in high colour intensity genotypes to specific carotenoid biosynthetic genes (Supplementary Table S4). Expression levels of the fruit-specific phytoene synthase-1 (*PSY-1*) were significantly higher in the ripe fruit of high-intensity lines (R1, R2, and R7), compared with the low- and medium-intensity lines (Fig. 4D).

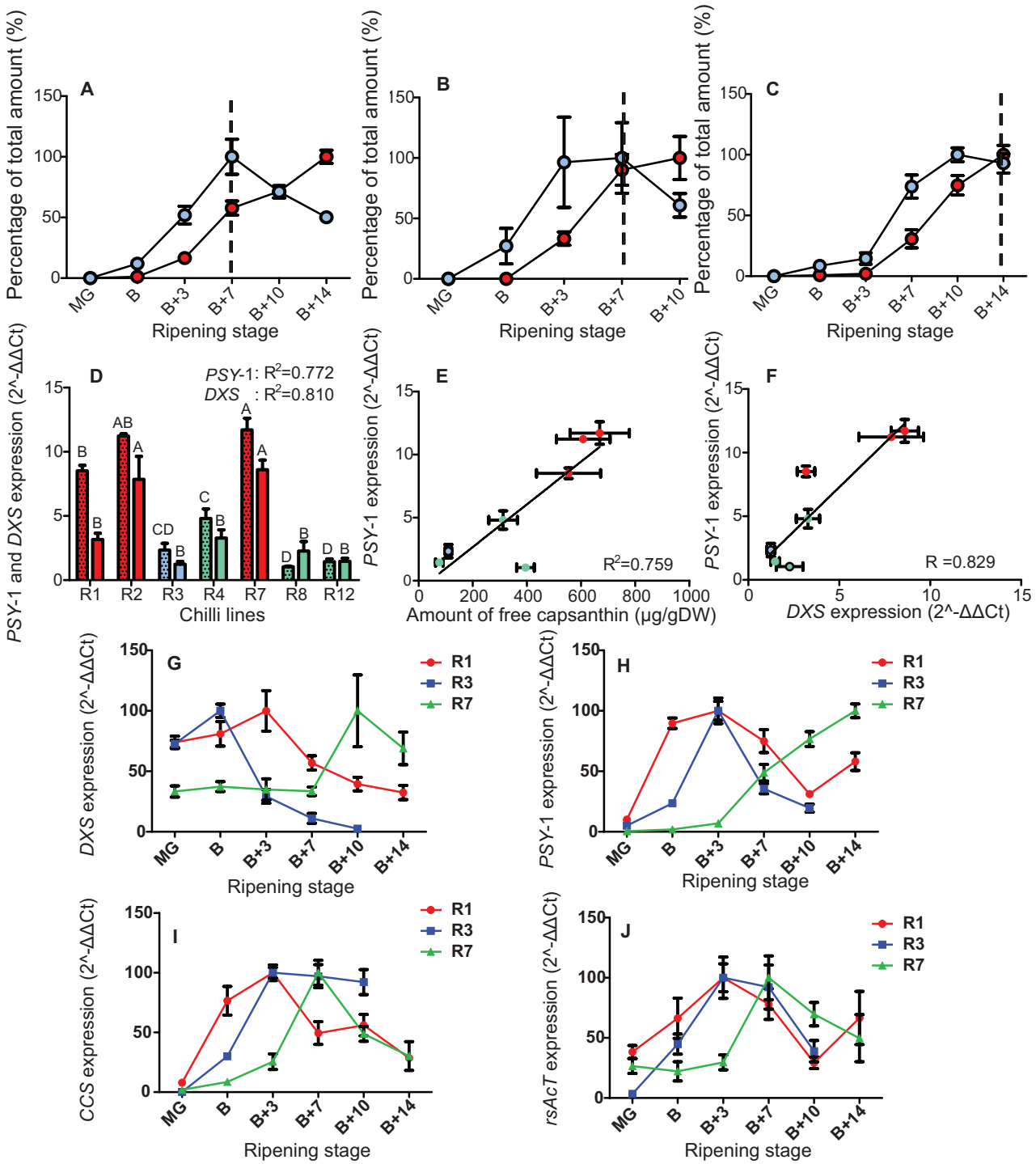

Fig. 4. Synthesis and accumulation of capsanthin and capsanthin esters during ripening, the relationship of phytoene synthase-1 (*PSY*-1) and 1-deoxy-D-xylulose 5-phopshate synthase (*DXS*) expression to colour intensity phenotype, and the expression of *DXS*, *PSY*-1, capsanthin capsorubin synthase (*CCS*), and a ripening-specific acyl transferase (*rsAcT*) during ripening. Free and esterified capsanthin amounts relative to levels of the highest abundance (=100%) throughout development were calculated for (A) R1, high intensity and fast ripening, (B) R3, low intensity and fast ripening, and (C) R7, high intensity and slow ripening. Expression levels of (D) *PSY*-1 (dotted) and *DXS* (clear) in ripe fruit. Linear regression of (E) *PSY*-1 expression and amount of free capsanthin and (F) *PSY*-1 expression and *DXS* expression were calculated. Key: blue, free capsanthin; red, capsanthin diesters; dotted line, transition from biosynthesis to accumulation based on a decline in free capsanthin accumulation when capsanthin diesters continue to increase (A–C) Red, high intensity; green, medium intensity; blue, low intensity; (D–F) A representation of the trend in phytoene synthase-1 (*PSY*-1) (H), 1-deoxy-D-xylulose 5-phosphate (*DXS*) (G), capsanthin capsorubin synthase (*CCS*) (I), and ripening-specific acyl transferase (*rsAcT*) (J). One-way ANOVA with Tukey post-hoc statistical analysis was carried out and lines were grouped based on their significance within the panel of lines ($P \leq 0.05$). Error bars represent ±SE ($n=3$).

Likewise, there was a strong positive correlation between *PSY*-1 expression and the amount of free capsanthin accumulated, with an R^2 value of 0.76 (Fig. 4E), as well as between *PSY*-1 and 1-deoxy-D-xylulose 5-phosphate synthase (*DXS*) expression (Fig. 4F), with an R^2 value of 0.83. Similarly, there was a positive correlation between *DXS* expression and high colour

intensity phenotype (R=0.81, P=0.03; Fig. 4D) and with the fruit-specific β-*CH2* and colour intensity phenotype; however, this gene was not as highly expressed as *PSY*-1 and *DXS* (R=0.77, P=0.04; Supplementary Fig. S2A). Interestingly, there was no correlation between gene expression of *CCS* and colour intensity, or any significant differences in *CCS* expression within the colour discovery panel (Supplementary Fig. S2B). *PSY*-1 and *DXS* gene products have been reported in tomato, pepper, and, recently, chilli pepper to have a strong influence over carotenoid formation in ripening fruit (Lois *et al.*, 2000; Huh *et al.*, 2001; Fraser *et al.*, 2002). Expression of *PSY*-1 and *DXS* were found to have significant correlation with the pigment content found across the intensity panel. These data suggest that the gene products modulate the supply of precursors into the pathway and are thus a progenitor of colour intensity.

The expression profile of *PSY*-1 during ripening reflected the rate of ripening (Fig. 4H). The fast-ripening lines (R1 and R3) showed a prominent peak in expression at the B+3 stage, whereas in the slow-ripening line (e.g. R7), it peaked at B+14, or possibly later. The expression profile in the two fast-ripening lines displayed that the high-intensity line (R1) had a broad peak in expression of *PSY*-1, spanning from B to B+7. In comparison, the low-intensity line (R3) had a narrower window of expression. The transcript levels between lines at specific stages of ripening reflected the qualitative trends previously described (Supplementary Fig. S2C–F). *DXS* transcripts showed peaks of expression at B+3 for R1, B for R3, and B+10 for R7 (Fig. 4G). Although no quantitative changes were observed between lines, the expression profile of *CCS* throughout ripening was determined (Fig. 4I). The two fast-ripening lines (R1 and R3) showed a peak in expression at the B+3 stage and the slow-ripening line (R7) showed a later peak in expression at around B+7. Comparison of the trends in *CCS* expression revealed that the high-intensity lines (R1 and R7) decreased at the later stages of ripening but the low-intensity line (R3) appeared to reach a peak at B+3 and then plateaud until B+10. At the B+7 and the B+10 stages of ripening, R1 and R7 had similar expression levels, whereas R3 was found to be expressed at a lower level (Supplementary Fig. S2J, K). Our expression data with *PSY*-2 suggested that this isoenzyme does not play a key role in ripening-related carotenoid accumulation.

These data correlate with the designation of phytoene synthase as having the most influence over the pathway. In tomato, flux control coefficients confirmed this hypothesis (Fraser *et al.*, 2002). The later stages of ripening showed that in the high-intensity lines free capsanthin was converted into capsanthin diesters. However, this was not accompanied by increased expression of the *CCS* gene. Thus, collectively, these data suggest that upstream gene products, such as DXS or PSY-1, or regulatory processes, such as feedback of free capsanthin to *CCS*, are responsible for high-level accumulation. *PSY*-1 expression was up-regulated at the onset of ripening in all lines. However, in addition to the quantitative increases in transcript levels, temporal and spatial changes were observed. For example, a comparison between two fast-ripening lines (R1 and R3), with high- and low-intensity phenotypes, respectively, showed that in both cases *PSY*-1 expression peaked at B+3. In the high-intensity line, R1, expression persisted throughout ripening compared with the limited period of maximal expression in the low-intensity line, R3. These results were further supported by immunoblotting that showed that PSY was more abundant in the R7 line than in R3. Enzyme activity assays showed that more PSY activity was present in the R7 line, confirming the integral role that PSY-1 plays in carotenoid accumulation in chilli (Fig. 6B; Supplementary Fig. S3G).

Pigment analysis revealed the key role that esterification plays in carotenoid accumulation/colour intensity (Hornero-Méndez and Mínguez-Mosquera, 2000). Based on the tomato *Pale yellow petal-1* (*PYP-1*) gene (Ariizumi *et al.*, 2014), an orthologue in chilli, denoted as a ripening-specific acyltransferase (*rsAcT*), has been identified. In tomato, the mutated *PYP-1* gene results in the absence of esterified xanthophylls in the flower (Ariizumi *et al.*, 2014). *rsAcT* also shares homology with *PES1* and *PES2*, the Arabidopsis orthologues, with 92% and 89% query coverage, respectively (Lippold *et al.*, 2012), but is more similar to *PYP-1* with 97% query coverage. The expression profile of *rsAcT* showed that it was expressed throughout ripening, with transcripts increasing in abundance with the onset of ripening and decreasing when ripening ceased (Fig. 4J). The two fast-ripening lines (R1 and R3) show that there was a peak in expression at around B+3. The slow-ripening line (R7) peaked later at B+7. When the levels of transcripts were directly compared between the lines, the B+3 stage of the high-intensity line showed significantly lower levels (Supplementary Fig. S2L). In contrast, the B+7 and B+10 stages showed no significant differences in the levels of *rsAcT* transcripts between the lines (Supplementary Fig. S2M, N). This indicated that the accumulation of free capsanthin, characteristic of the high-intensity lines, could be explained by inefficient esterification in the plastid, resulting in a pool of free carotenoids accumulating prior to esterification. Further studies, such as colour complementation using bacterial systems, or virus-induced gene silencing, could potentially be used to characterize carotenoid esterification further and the potential role of these acyl transferases.

Carotenoids are sequestered differentially in high- and low-intensity lines

Chromoplast fractionation and carotenoid location in subplastid fractions

In order to determine what ultrastructural features sequestrate carotenoids, subplastid fractionation was carried out on ripe fruit (Fig. 5A). The fractionation was applied to two extreme genotypes, R3 representing the low colour intensity population, compared with the high-intensity R7 line. The PG fractions (F1–F2) were denser and visually a darker red in the R7 line, compared with the PG fractions in the R3 line. Positioned in the middle of the gradient was a collection of dense particulate layers (F6–F22). The first particulate layer was designated membrane I (MI), (F6–F11). In the R3 extract, this band had an orange hue, but was found to have a red hue in the R7 extract. Located below MI were a collection of vertical, threadlike structures (F12–F16), designated the fibrillar region. This region was denser in R7 compared with R3 (Fig. 5A). Membrane II (MII) was positioned under the fibrils (F16–F22) and the stromal fractions were

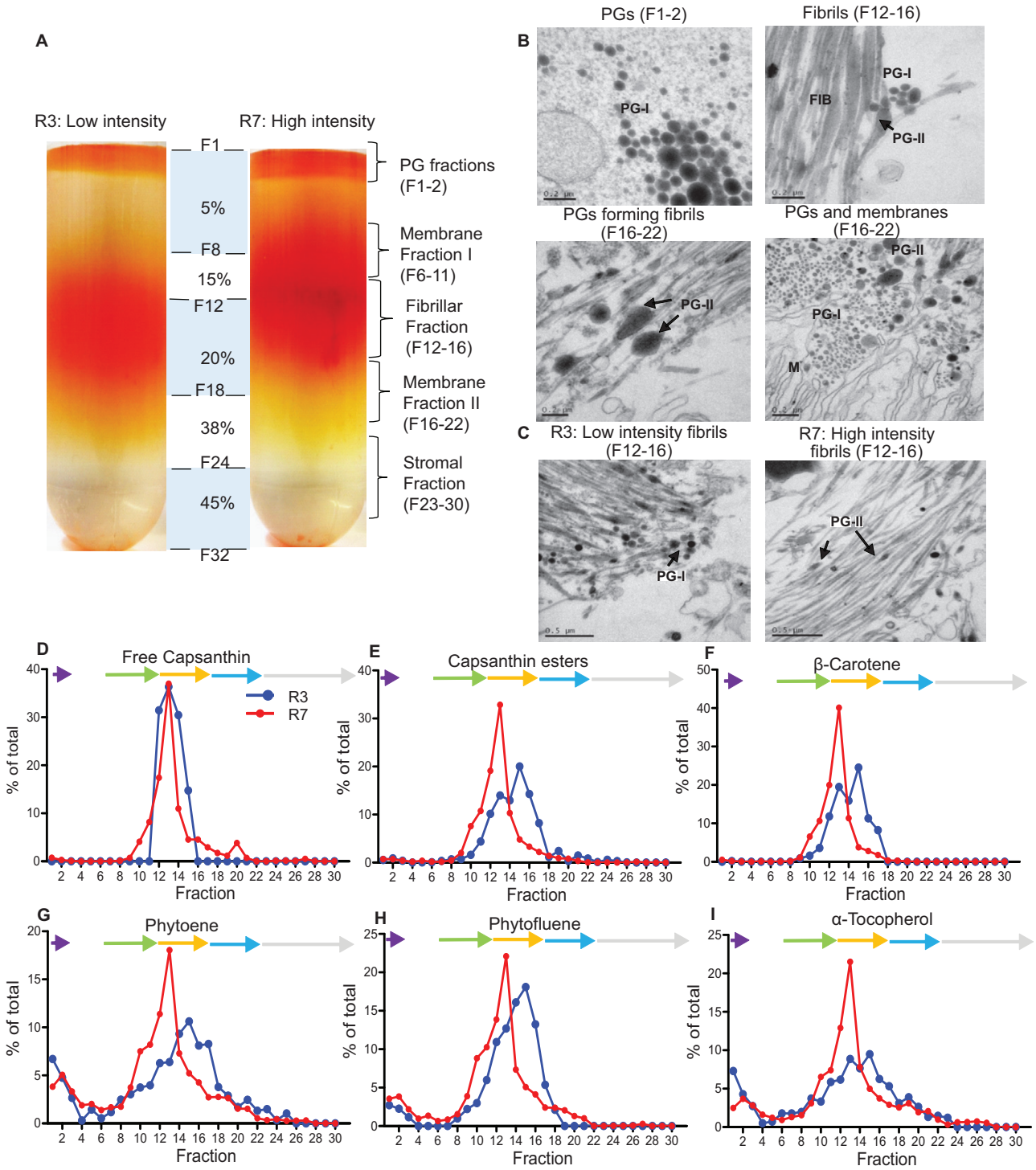

Fig. 5. Subplastid fractionation of red chilli pepper from a low- (R3) and high- (R7) intensity line. (A) Chromoplasts were extracted from ripe fruit (20 g) and separated on a sucrose gradient. F1+F8 had a gradient of 5%, F9–F12 15%, F13–18 20%, F21–24 38%, and F25–32 45% sucrose (w/v) as described in the Materials and methods. (B) Representative TEMs on the fractions of ripe chilli fruit: free plastoglobuli (PGs: F1–F2), fibrils (F12–F16), and fibril formation from PGs and PGs and membrane systems (MII: F16–F22). (C) Representative TEMs comparing the fibril fractions of a low- (R3) and high-intensity line (R7) (F12-F16). Key: M, membranes; PG-I, early stage plastoglobule; PG-II, late stage plastoglobule; FIB, fibril. The pigments in each fraction were extracted and subjected to HPLC-PDA, and the percentage of each compound across the gradient was calculated (total amount of each compound=100%). A representative portion of the most abundant pigments is shown (D–I). The arrows represent the subplastid fractions; purple, plastoglobule; green, membrane fraction I; orange, fibril; blue, membrane fraction II; grey, stroma.

located underneath MII (F23–F30). This was different from the fractionation banding observed in tomato fruit which consisted of a PG layer and then a membrane layer (16–24), with two distinct regions (Nogueira *et al*., 2013). Another striking difference observed in tomato was the presence of crystalline aggregates associated with the membrane layers instead of a fibril fraction, thus highlighting the differences in sequestration mechanisms between tomato and *Capsicum* (Nogueira *et al*., 2013).

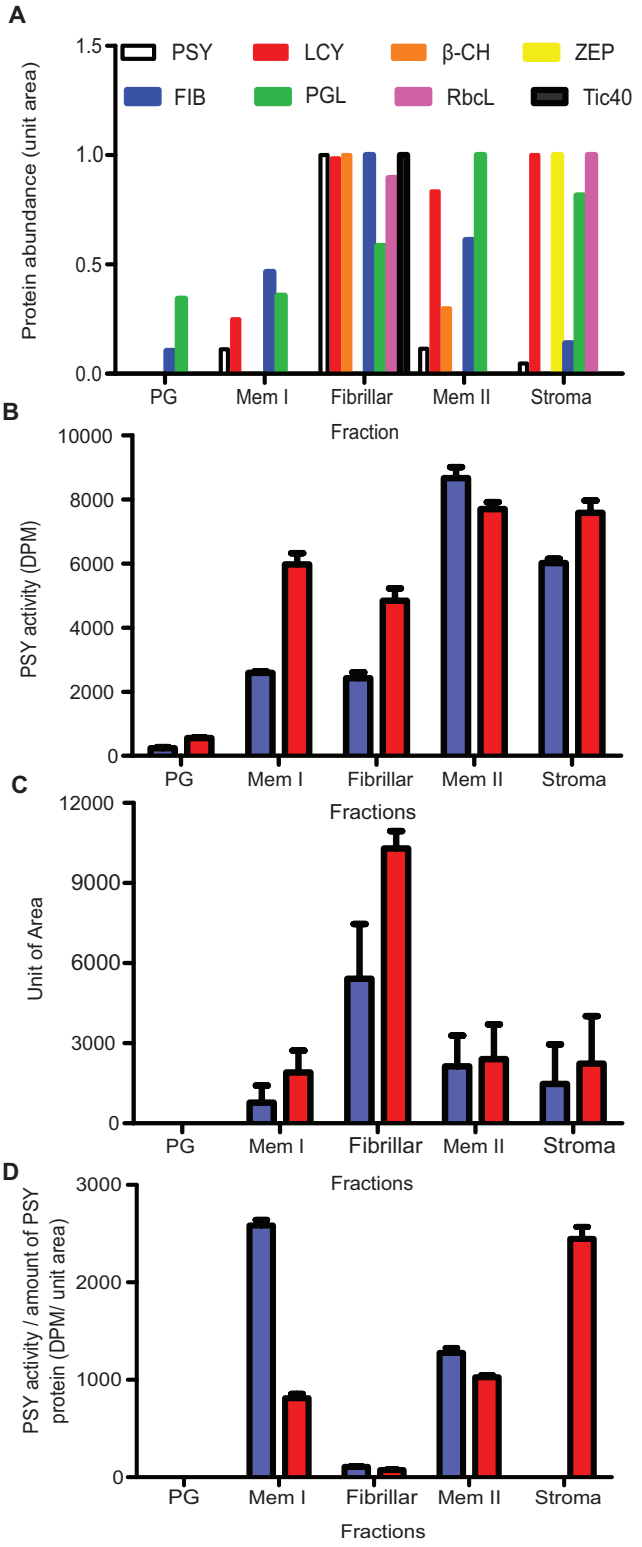

Fig. 6. Subplastidial localization of carotenoid biosynthesis enzymes and biomarkers. (A) Abundance of carotenoid biosynthetic enzymes and biomarkers throughout the gradient. (B) PSY activity, (C) quantification of PSY protein abundance over two rounds of immunoblotting, and (D) PSY activity per amount of PSY-1 protein. Abundance was quantified using scanned images of the developed membranes in ImageJ. See Supplementary Table S6 for one-way ANOVA on PSY activity. Abbreviations: PSY, phytoene synthase; LCY, lycopene β-cyclase; β-CH, β-carotene hydroxylase; ZEP, zeaxanthin epoxidase; FIB, fibrillin; PGL, plastoglobulin; RbcL, Rubisco large subunit; Tic40, chloroplast inner envelope membrane translocon complex protein.

Antibodies to plastid biomarkers, were used to aid the characterization/identification of the fractions (Fig. 6A). Plastoglobulin and fibrillin were located throughout the gradient, with the highest abundance found in MII and the fibrils, respectively. This was similar to tomato as plastoglobulin was found in the PGs, lower membrane layer, and stroma (Nogueira *et al.*, 2013). RbcL, a traditional stromal biomarker, was located in the stroma and fibrils, and Tic40, a designated chloroplast inner envelope membrane translocon complex protein, was located in the fibrils. However, this differed from tomato as RbcL and Tic40 were located in the stroma (Nogueira *et al.*, 2013). The distribution of carotenoids across the gradient within the subplastid structures was significantly higher for all carotenoids and α-tocopherol in the R7 line compared with the R3 line. The percentage of each compound throughout the gradient was analysed to see where specific compounds were predominantly sequestered within the chromoplast (total amount of each compound=100%). In R7, the fibril fraction contained the most pigments, while the R3 line displayed a split distribution of carotenoids across the fibrils and MII (Fig. 5D–I; Supplementary Table S5 shows the standard error of the different fraction designations). Interestingly, this differed from tomato where the high carotenoid-producing transgenic line accumulated pigments over two dense sectors but control accumulated in the equivalent of MII (Nogueira *et al.*, 2013). The membrane fractions, specifically the fibrils, contained the highest proportion of pigments throughout the gradient. Capsanthin, antheraxanthin, zeaxanthin, capsorubin, and β-carotene were allocated to the fibrillar fractions at 40–50% in the R7 line (Fig. 5; Supplementary Fig. S3A–F). This was also true in R3 for free capsanthin and zeaxanthin as well as their corresponding esters. When looking at the amount of compound (carotenoid) accumulated, in most cases there was over double the amount of carotenoids present, with the red carotenoid esters, capsanthin and capsorubin, being 5- and 8-fold in the high-intensity line. The fact that the capsanthin diesters were distributed at a higher amount in the fibrillar fractions in the high-intensity line could be a contributing factor to their difference in colour intensity phenotype, whereby high levels of capsanthin diesters initiate more fibril formation. The differences observed in tomato and *Capsicum* in reference to preferential accumulation of pigments in the chromoplast reflect the different sequestration mechanisms at play. The high carotenoid-producing transgenic tomato (Nogueira *et al.*, 2013; ~3 mg g^{-1} DW) is similar to the *Capsicum* low-intensity line when pigments are accumulating at lower levels and so remain associated with membranes and PGs. The high-intensity line (~9 mg g^{-1} DW) displays a clear ultrastructural adaptation to higher levels of carotenoids by preferentially accumulating them in the fibrils, as opposed to the membranes.

Phytoene (2–7%), α-tocopherol (2–7%), and phytofluene (2–3%) were found in the PG fractions. The R3 line was found to allocate more phytoene and α-tocopherol to the PGs when compared with R7 (Fig. 5G, I). The R3 line was found to contain more carotenoids associated with the PGs (phytoene, α-tocopherol, and phytofluene) in MII. The PGs preferentially accumulate phytoene, phytofluene, and α-tocopherol. Other coloured carotenoids, such as capsanthin

esters and β-carotene, were present, but at a low level compared with other fractions (Fig. 5). In the low-intensity line, a greater proportion of phytoene and phytofluene was found. Collectively, these data suggest that PGs serve as a sink to deposit excess phytoene and phytofluene, perhaps as a regulatory mechanism through compartmentalization, as revealed previously (Nogueira *et al.*, 2013).

Carotenoid biosynthetic enzymes associated with subplastid structures

The carotenoid biosynthetic enzymes PSY, LCY, and β-CH were found in all the membrane fractions and in part the stromal fraction (except β-CH). ZEP, which was reported to be located in the stromal side of the thylakoids (Hieber *et al.*, 2000), was found in stromal fractions. PSY activity was measured throughout the gradient to ascertain its subplastidial location and compare how enzyme activity differed in a low- and high-intensity line (Fig. 6B, D). Activity was predominantly located in MII and the stromal fractions. In all fractions, excluding MII, R7 had significantly more activity compared with R3 (Supplementary Table S6). This was supported by the presence of more PSY protein in R7 of the MI, fibril, MII, and stroma when compared with R3 (Fig. 6C; Supplementary Fig. S3G). Although the PSY protein was most abundant in the fibrillar fraction, on an activity per amount of PSY protein basis, the fibril fraction had the lowest activity, with the highest specific activity being in MI and stroma. R3 exhibited greater specific activity than R7 in MI, but the opposite was true for the stroma. Based on this collective evidence, we hypothesize that MII is the predominant location for synthesis, from which the PG blisters from the membrane as proposed in Austin *et al.* (2006) and Camara and Brangeon (1981). Studies on the localization, activity, and abundance of the carotenoid biosynthetic enzymes across different subplastid components has also provided insight into how the carotenoids are synthesized and stored. The finding that the PSY protein was most abundant in the fibrillar fraction, but more active in the membrane fractions and stroma, suggests that the membranes are sites for carotenoid synthesis, but its presence in the stroma also indicated that the PSY enzyme is not integral (Fig. 6D). These data are in agreement with other reports (Dogbo *et al.*, 1987; Fraser *et al.*, 1994). The abundance of the PSY protein in the fibrillar fractions is indicative of the complex membranous systems involved in the orchestration of fibril formation, and that the location of the enzyme is fundamental to the optimal active state. It could also be postulated that the inactive and/or reduced specific PSY activity/protein could even contribute to the macromolecular structure of the fibril. Previous studies in maize found that PSY was located in different subplastid locations depending on the isoform. The isoform related to coloured kernels was located in stroma and associated with membranes (Shumskaya *et al.*, 2012).

An interesting discovery was the low levels of carotenogenic proteins (PSY, LCY, β-CH, and ZEP) present in the PGs. This is contradictory to the results from proteomic studies whereby the presence in PGs of some carotenoid biosynthesis enzymes (ZDS, LCY, and β-CH) was shown (Austin *et al.*, 2006; Ytterberg *et al.*, 2006; Vidi *et al.*, 2006). These enzymes may be incorporated into PGs during the blistering process as a result of being present in the synthesis membranes, but it is imperative to highlight that the presence of the protein does not convey that it was active, as seen with PSY in the fibrils.

Cellular structures observed in subplastidial fractions

TEM micrographs of the fractions also showed distinct structures present in the fractions (Fig. 5B). From the micrographs, it was observed that fibrils were not isolated and were found to be associated with the PGs, incorporated into complex membrane and PG systems (Fig. 5B). This finding implies that the fibrils originate from the PGs. This has also been observed in previous studies on whole tissue not isolated fractions (Simpson and Lee, 1976). Austin *et al.* (2006) also report PGs forming clusters, whereby the PGs can blister from the thylakoid membrane or from another PG. This strongly supports the notion that fibrils could arise from PGs in the chilli pepper chromoplast. Previous research has implied that the PGs are thought to be initiation sites for fibril formation, and the presence of bicyclic diesters at a critical level has been suggested as essential for initiation of the fibril formation from the PGs (Simpson and Lee, 1976; Simpson *et al.*, 1977; Deruère *et al.*, 1994). This was also visualized in the present study whereby the PGs can be found in an intermediate form (Fig. 5B, PG-II) and could explain the finding that all the carotenoids examined were predominantly distributed into fibrillar fractions. If this is the case and the formation of fibrils is dependent on the composition and amount of carotenoids present in the PGs, a comparison between the low- and high-intensity lines could show the PGs at different stages of development (van Wijk and Kessler, 2017; Fig. 6). As previously shown, a higher percentage of carotenoids and carotenoid esters were distributed in the PGs in the low-intensity line, R3 (Fig. 5D–I). In the R3 line, the PGs were in early stages of development, characterized by phytoene and α-tocopherol having a larger percentage of the total pigments, as well as showing more PGs with a globular shape (Fig. 5C, PG-I). R7, however, showed much later stages of development, perhaps after fibril formation was initiated, with the presence of more PG-II structures (Fig. 5C). The presence of other carotenoids and a higher amount and composition of esters seen here may be the progenitor and influential contributor to fibril formation (Deruère *et al.*, 1994). Evidence suggests a major role for fibrillin in the transformation of PGs into fibrils (Deruère *et al.*, 1994). This further supports the discovery that the high-intensity line (R7) accumulates a larger amount of fibrils, demonstrated with a larger fibrillar band, when compared with R3, as this line had a considerably higher total carotenoid content with particular emphasis on capsanthin diester accumulation. The PG-I then elongates in to PG-II as the fibril develops, and it is proposed that additional carotenoids and lipids are required for fibril development, and we speculate that their presence could be found in MI on the fractionation gradient, between the PGs and fibrils (Fig. 5B; PG-II). The similarity of the protein profiles of fibrillin and PG-1 within the fractions could also suggest the formation of PGs to fibrils. The formation of PGs and fibrils occurs in a complex membrane system; the PGs and fibrils should therefore not be imagined as single entities but continuous systems

for production and sequestration. The presence of plastoglobulin predominantly in MII supports this view, as plastoglobulin is being recruited to the synthesis membranes to initiate PG blistering from the membrane. Our findings support previous studies and speculation that in chilli pepper the PG structures serve as an intermediate storage structure and not the final destination of storage (Simpson and Lee, 1976; Prebeg *et al*., 2006*a*, *b*); therefore, it was not surprising that plastoglobulin was ubiquitous to these fractions.

In summary, the intensity of fruit colour is a consumer-driven, commercial trait for chilli pepper. Red fruit coloration is conferred by carotenoids, particularly capsanthin and its derivatives. The present study has revealed the complexity of carotenoid formation in this crop plant. The correlation of ripening and carotenoid formation suggests a role for an overarching developmental master regulator in this non-climatic fruit. The pathway itself has elements of transcriptional and post-transcriptional regulation, particularly at the stage of phytoene synthesis. Our detailed carotenoid determinations, transcript analysis, enzyme levels and activity, and cellular analysis have led to the postulation of distinct carotenoid synthesis and accumulation phases. In addition, the data imply that altered metabolite levels are the progenitor of specialized ultrastructural storage sites. Collectively, the underpinning data acquired in the present approach have generic implications for future crop improvement programmes directed towards enhanced quality traits, such as colour in fleshy fruits. However, it is clear that direct translation of findings from tomato (the fruit model) to other fleshy fruits is an unrealistic interpretation, and dedicated studies, particularly with respect to specialized metabolism, are warranted.

Supplementary data

Supplementary data are available at *JXB* online.

Fig S1. Summary of carotenoid content in ripe fruit.

Fig S2. Direct comparisons of gene expression analysis: *PSY*-1, *PSY*-2, DXS, and acyl transferase.

Fig S3. Distribution of pigments and subplastid localization of PSY across the gradient in a low- and high-intensity line.

Table S1. Colour intensity phenotypes of the *Capsicum annuum* colour discovery panel used in this study.

Table S2. Carotenoid and carotenoid esters identified in red ripe chilli pepper fruit using HPLC-PDA and LC-MS.

Table S3. Carotenoid content throughout ripening in eight selected lines.

Table S4. Primers designed for qPCR of carotenoid biosynthesis-related genes.

Table S5. Standard error of the mean for the percentage of each carotenoid across the gradient.

Table S6. One-way ANOVA for phytoene synthase activity (DPM) and phytoene synthase activity/molecule of enzyme (DPM/unit area).

Acknowledgments

Financial support for this study was provided through the BBSRC Syngenta Ltd iCASE award BB/1015590/1. Professor Bramley is thanked for his critical evaluation of the work.

Author contributions

HMB performed the experimental work; HMB, DVR, CB, EMAE, and PDF designed the research programme; PDF secured funds; and all authors commented on the results and contributed to the manuscript.

References

Alder A, Jamil M, Marzorati M, Bruno M, Vermathen M, Bigler P, Ghisla S, Bouwmeester H, Beyer P, Al-Babili S. 2012. The path from β-carotene to carlactone, a strigolactone-like plant hormone. Science **335**, 1348–1351.

Ariizumi T, Kishimoto S, Kakami R, *et al*. 2014. Identification of the carotenoid modifying gene PALE YELLOW PETAL 1 as an essential factor in xanthophyll esterification and yellow flower pigmentation in tomato (*Solanum lycopersicum*). The Plant Journal **79**, 453–465.

Austin JR 2nd, Frost E, Vidi PA, Kessler F, Staehelin LA. 2006. Plastoglobules are lipoprotein subcompartments of the chloroplast that are permanently coupled to thylakoid membranes and contain biosynthetic enzymes. The Plant Cell **18**, 1693–1703.

Baenziger PS, Mumm RH, Bernando R, Brummer EC, Langride P, Simon P, Smith S. 2017. Council for Agricultural Science and Technology (CAST). Plant Breeding and Genetics. Issue Paper 57. Ames, IA: CAST.

Bouvier F, D'harlingue A, Backhaus RA, Kumagai MH, Camara B. 2000. Identification of neoxanthin synthase as a carotenoid cyclase paralog. European Journal of Biochemistry **267**, 6346–6352.

Breithaupt DE, Schwack W. 2000. Determination of free and bound carotenoids in paprika (*Capsicum annuum* L.) by LC/MS. European Food Research and Technology **211**, 52–55.

Britton G, Liaaen-Jensen S, Pfander H, eds.2004. Carotenoids handbook.. Basel: Birkhauser Verlag.

Camara B, Brangeon J. 1981. Carotenoid metabolism during chloroplast to chromoplast transformation in *Capsicum annuum* fruit. Planta **151**, 359–364.

Camara B, Hugueney P, Bouvier F, Kuntz M, Monéger R. 1995. Biochemistry and molecular biology of chromoplast development. International Review of Cytology **163**, 175–247.

Cervantes-Paz B, Yahia EM, de Jesús Ornelas-Paz J, Victoria-Campos CI, Ibarra-Junquera V, Pérez-Martínez JD, Escalante-Minakata P. 2014. Antioxidant activity and content of chlorophylls and carotenoids in raw and heat-processed Jalapeño peppers at intermediate stages of ripening. Food Chemistry **146**, 188–196.

Demmig-Adams B, Adams WW 3rd. 2002. Antioxidants in photosynthesis and human nutrition. Science **298**, 2149–2153.

Deruère J, Römer S, d'Harlingue A, Backhaus RA, Kuntz M, Camara B. 1994. Fibril assembly and carotenoid overaccumulation in chromoplasts: a model for supramolecular lipoprotein structures. The Plant Cell **6**, 119–133.

Dogbo O, Bardat F, Laferriere A, Quennemet J, Brangeon J, Camara B. 1987. Metabolism of plastid terpenoids. I. Biosynthesis of phytoene in plastid stroma isolated from higher plants. Plant Science **49**, 89–101.

Enfissi EM, Barneche F, Ahmed I, *et al*. 2010. Integrative transcript and metabolite analysis of nutritionally enhanced DE-ETIOLATED1 downregulated tomato fruit. The Plant Cell **22**, 1190–1215.

Enfissi EM, Nogueira M, Bramley PM, Fraser PD. 2017. The regulation of carotenoid formation in tomato fruit. The Plant Journal **89**, 774–788.

Fraser PD, Bramley PM. 2004. The biosynthesis and nutritional uses of carotenoids. Progress in Lipid Research **43**, 228–265.

Fraser PD, Romer S, Shipton CA, Mills PB, Kiano JW, Misawa N, Drake RG, Schuch W, Bramley PM. 2002. Evaluation of transgenic tomato plants expressing an additional phytoene synthase in a fruit-specific manner. Proceedings of the National Academy of Sciences, USA **99**, 1092–1097.

Fraser PD, Schuch W, Bramley PM. 2000. Phytoene synthase from tomato (*Lycopersicon esculentum*) chloroplasts—partial purification and biochemical properties. Planta **211**, 361–369.

Fraser PD, Truesdale MR, Bird CR, Schuch W, Bramley PM. 1994. Carotenoid biosynthesis during tomato fruit development (evidence for tissue-specific gene expression). Plant Physiology **105**, 405–413.

Giuffrida D, Dugo P, Torre G, Bignardi C, Cavazza A, Corradini C, Dugo G. 2013. Characterization of 12 *Capsicum* varieties by evaluation of their carotenoid profile and pungency determination. Food Chemistry **140**, 794–802.

Giuliano G. 2017. Provitamin A biofortification of crop plants: a gold rush with many miners. Current Opinion in Biotechnology **44**, 169–180.

Gómez-García Mdel R, Ochoa-Alejo N. 2013. Biochemistry and molecular biology of carotenoid biosynthesis in chili peppers (*Capsicum* spp.). International Journal of Molecular Sciences **14**, 19025–19053.

Guzman I, Hamby S, Romero J, Bosland PW, O'Connell MA. 2010. Variability of carotenoid biosynthesis in orange colored *Capsicum* spp. Plant Science **179**, 49–59.

Hieber AD, Bugos RC, Yamamoto HY. 2000. Plant lipocalins: violaxanthin de-epoxidase and zeaxanthin epoxidase. Biochimica et Biophysica Acta **1482**, 84–91.

Hornero-Méndez D, Mínguez-Mosquera MI. 1994. Changes in carotenoid esterification during fruit ripening of *Capsicum annuum* Cv. Bola. Journal of Agricultural and Food Chemistry **42**, 640–644.

Hornero-Méndez D, Mínguez-Mosquera MI. 2000. Xanthophyll esterification accompanying carotenoid overaccumulation in chromoplast of *Capsicum annuum* ripening fruits is a constitutive process and useful for ripeness index. Journal of Agricultural and Food Chemistry **48**, 1617–1622.

Hugueney P, Bouvier F, Badillo A, Quennemet J, d'Harlingue A, Camara B. 1996. Developmental and stress regulation of gene expression for plastid and cytosolic isoprenoid pathways in pepper fruits. Plant Physiology **111**, 619–626.

Huh JH, Kang BC, Nahm SH, Kim S, Ha KS, Lee MH, Kim BD. 2001. A candidate gene approach identified phytoene synthase as the locus for mature fruit color in red pepper (*Capsicum* spp.). Theoretical and Applied Genetics **102**, 524–530.

Ji K, Kai W, Zhao B, *et al*. 2014. *SlNCED1* and *SlCYP707A2*: key genes involved in ABA metabolism during tomato fruit ripening. Journal of Experimental Botany **65**, 5243–5255.

Kachanovsky DE, Filler S, Isaacson T, Hirschberg J. 2012. Epistasis in tomato color mutations involves regulation of *phytoene synthase 1* expression by *cis*-carotenoids. Proceedings of the National Academy of Sciences, USA **109**, 19021–19026.

Kilcrease J, Collins AM, Richins RD, Timlin JA, O'Connell MA. 2013. Multiple microscopic approaches demonstrate linkage between chromoplast architecture and carotenoid composition in diverse *Capsicum annuum* fruit. The Plant Journal **76**, 1074–1083.

Kilcrease J, Rodriguez-Uribe L, Richins RD, Arcos JM, Victorino J, O'Connell MA. 2015. Correlations of carotenoid content and transcript abundances for fibrillin and carotenogenic enzymes in *Capsicum annum* fruit pericarp. Plant Science **232**, 57–66.

Kim S, Park M, Yeom SI, *et al*. 2014. Genome sequence of the hot pepper provides insights into the evolution of pungency in Capsicum species. Nature Genetics **46**, 270–278.

Lefebvre V, Kuntz M, Camara B, Palloix A. 1998. The capsanthin-capsorubin synthase gene: a candidate gene for the y locus controlling the red fruit colour in pepper. Plant Molecular Biology **36**, 785–789.

Lippold F, vom Dorp K, Abraham M, *et al*. 2012. Fatty acid phytyl ester synthesis in chloroplasts of *Arabidopsis*. The Plant Cell **24**, 2001–2014.

Lois LM, Rodríguez-Concepción M, Gallego F, Campos N, Boronat A. 2000. Carotenoid biosynthesis during tomato fruit development: regulatory role of 1-deoxy-D-xylulose 5-phosphate synthase. The Plant Journal **22**, 503–513.

Lu S, Van Eck J, Zhou X, *et al*. 2006. The cauliflower Or gene encodes a DnaJ cysteine-rich domain-containing protein that mediates high levels of beta-carotene accumulation. The Plant Cell **18**, 3594–3605.

Moise AR, Al-Babili S, Wurtzel ET. 2014. Mechanistic aspects of carotenoid biosynthesis. Chemical Reviews **114**, 164–193.

Nogueira M, Berry H, Nohl R, Klompmaker M, Holden A, Fraser PD. 2016. Subchromplast fractionation protocol for different solanaceae fruit species. Bio-Protocol **6**, e1861.

Nogueira M, Mora L, Enfissi EM, Bramley PM, Fraser PD. 2013. Subchromoplast sequestration of carotenoids affects regulatory mechanisms in tomato lines expressing different carotenoid gene combinations. The Plant Cell **25**, 4560–4579.

Perez-Fons L, Steiger S, Khaneja R, Bramley PM, Cutting SM, Sandmann G, Fraser PD. 2011. Identification and the developmental formation of carotenoid pigments in the yellow/orange Bacillus spore-formers. Biochimica et Biophysica Acta **1811**, 177–185.

Prebeg T, Ljubesic N, Wrischer M. 2006*a*. Chromoplast biogenesis in *Chelidonium majus* petals. Acta Societatis Botanicorum Poloniae **75**, 107–112.

Prebeg T, Ljubešić N, Wrischer M. 2006*b*. Differentiation of chromoplasts in *Cucumis sativus* petals. International Journal of Plant Sciences **167**, 437–445.

Qin C, Yu C, Shen Y, *et al*. 2014. Whole-genome sequencing of cultivated and wild peppers provides insights into Capsicum domestication and specialization. Proceedings of the National Academy of Sciences, USA **111**, 5135–5140.

Rodriguez-Concepcion M, Avalos J, Bonet ML, *et al*. 2018. A global perspective on carotenoids: metabolism, biotechnology, and benefits for nutrition and health. Progress in Lipid Research **70**, 62–93.

Rodriguez-Uribe L, Guzman I, Rajapakse W, Richins RD, O'Connell MA. 2012. Carotenoid accumulation in orange-pigmented *Capsicum annuum* fruit, regulated at multiple levels. Journal of Experimental Botany **63**, 517–526.

Schweiggert U, Kammerer DR, Carle R, Schieber A. 2005. Characterization of carotenoids and carotenoid esters in red pepper pods (*Capsicum annuum* L.) by high-performance liquid chromatography/atmospheric pressure chemical ionization mass spectrometry. Rapid Communications in Mass Spectrometry **19**, 2617–2628.

Shumskaya M, Bradbury LM, Monaco RR, Wurtzel ET. 2012. Plastid localization of the key carotenoid enzyme phytoene synthase is altered by isozyme, allelic variation, and activity. The Plant Cell **24**, 3725–3741.

Simkin AJ, Gaffé J, Alcaraz JP, Carde JP, Bramley PM, Fraser PD, Kuntz M. 2007. Fibrillin influence on plastid ultrastructure and pigment content in tomato fruit. Phytochemistry **68**, 1545–1556.

Simpson DJ, Baqar MR, Lee TH. 1977. Fine structure and carotenoid composition of the fibrillar chromplasts of *Asparagus officinalis* L. Annals of Botany **41**, 1101–1108.

Simpson DJ, Lee TH. 1976. The fine structure and formation of fibrils of *Capsicum annuum* L. chromoplasts. Zeitschrift fur Pflanzenphysiologie **77**, 127–138.

Story EN, Kopec RE, Schwartz SJ, Harris GK. 2010. An update on the health effects of tomato lycopene. Annual Review of Food Science and Technology **1**, 189–210.

Thorup TA, Tanyolac B, Livingstone KD, Popovsky S, Paran I, Jahn M. 2000. Candidate gene analysis of organ pigmentation loci in the Solanaceae. Proceedings of the National Academy of Sciences, USA **97**, 11192–11197.

van Wijk KJ, Kessler F. 2017. Plastoglobuli: plastid microcompartments with integrated functions in metabolism, plastid developmental transitions, and environmental adaptation. Annual Review of Plant Biology **68**, 253–289.

Vidi PA, Kanwischer M, Baginsky S, Austin JR, Csucs G, Dörmann P, Kessler F, Bréhélin C. 2006. Tocopherol cyclase (VTE1) localization and vitamin E accumulation in chloroplast plastoglobule lipoprotein particles. Journal of Biological Chemistry **281**, 11225–11234.

Vishnevetsky M, Ovadis M, Vainstein A. 1999. Carotenoid sequestration in plants: the role of carotenoid-associated proteins. Trends in Plant Science **4**, 232–235.

Welsch R, Zhou X, Yuan H, *et al*. 2018. Clp protease and OR directly control the proteostasis of phytoene synthase, the crucial enzyme for carotenoid biosynthesis in *Arabidopsis*. Molecular Plant **11**, 149–162.

Wurtzel ET. 2019. Changing form and function through carotenoids and synthetic biology. Plant Physiology **179**, 830–843.

Ytterberg AJ, Peltier JB, van Wijk KJ. 2006. Protein profiling of plastoglobules in chloroplasts and chromoplasts. A surprising site for differential accumulation of metabolic enzymes. Plant Physiology **140**, 984–997.